Results: A total of 715 individuals who experienced atrial fibrillation or atrial flutter were matched to 72,215 controls. To account for the potential unmeasured confounders, we identified nitrate users in the same cohort as an active comparator. After adjustment, new use of nicorandil was found to be associated with increased risk for atrial
fibrillation or atrial flutter (odds ratio [OR], 2.34; 95% CI 1.07-5.13) compared to nitrate use. Activation of potassium channel shortens atrial action potential duration (APD), which subsequently perpetuates AF. Dysfunction of mutated sarcKATP channels in atrial cells may lead to electrical instability and atrial fibrillation. We found expression of KATP in human atrial tissues. Furthermore, nicorandil directly shortened APD and the QT interval of cultured induced pluripotent stem cell (iPSC) derived cardiomyocytes (iPSC-CMs).
Conclusion: Use of nicorandil, especially new use, was found to be associated with increased risk of AF or AFL. We also first showed the expression of KATP in human atria and use of nicorandil may promote or increase the risk of AF through activation of KATP and shortening of atrial APD.

B-PO02-019

MITOCHONDRIAL CONNEXIN43 IS INVOLVED IN THE OCCURRENCE OF ARRHYTHMIAS WITH MODULATION OF MITOCHONDRIAL K_{ATP} CHANNELS

Wakako Satoh, Haruka Sato MD, PhD, Kazunori Kumasaka, Chiyohiko Shindoh MD, PhD and Masahito Miura MD, PhD

Background: Connexin43 (Cx43) forms gap junctional channels in cardiac ventricles and exits as hemichannels in the inner mitochondrial membrane (mCx43).
Objective: To examine whether mCx43 and mitochondrial K_{ATP} channels (mK_{ATP}) affect the occurrence of arrhythmias.
Methods: To generate cardiac-specific Cx43-deficient (*Cx43*$^{-/-}$) mice, *Cx43*$^{flox/flox}$ mice were crossed with α-myosin heavy chain (*Myh6*)-*cre*$^{+/-}$ mice. The resulting offspring, *Cx43*$^{-/-}$-mice and their littermates (*Cx43*$^{+/+}$-mice) were used. Trabeculae were dissected from ventricles. Force was measured with a silicon strain gauge, Ca^{2+} within the mitochondria (Ca_m) with rhod-2, intracellular Ca^{2+} (Ca_i) with microinjected fura-2 (22°C). The minimal extracellular Ca^{2+} concentration (Cao_{min}), at which arrhythmias were induced by electrical stimulation, was determined. Using isolated single ventricular myocytes, mitochondrial membrane potential ($\Delta\Psi_m$) was estimated with tetramethylrhodamine methylester (TMRM), ROS production with 2',7'-dichlorofluorescein (DCF), and Ca^{2+} spark frequency with fluo-4 and confocal microscopy.
Results: Most of *Cx43*$^{-/-}$-mice died within 8 weeks ($p<0.01$). Cx43 was present in the inner mitochondrial membrane in *Cx43*$^{+/+}$-mice but not in *Cx43*$^{-/-}$-mice. Developed force and Ca_i transients by 0.5 Hz electrical stimulation showed no difference between *Cx43*$^{-/-}$- and *Cx43*$^{+/+}$-mice ($n=7$). The Cao_{min} in *Cx43*$^{-/-}$-mice was lower than that in *Cx43*$^{+/+}$-mice ($n=5$, $p<0.01$) and was increased by diazoxide (DZX, $n=4$, $p<0.05$), suggesting that arrhythmogenesis is increased in *Cx43*$^{-/-}$-mice and is suppressed by DZX. Ca^{2+} spark frequency and DCF oxidation rate in *Cx43*$^{-/-}$-mice were higher ($p<0.01$) and were decreased by DZX ($p<0.01$). TMRM fluorescence was decreased after 1 Hz stimulation in *Cx43*$^{-/-}$-mice, and it was increased by DZX ($p<0.01$) and was decreased by 5-hydroxydecanoic acid ($p<0.01$). Rhod-2 signal was increased in *Cx43*$^{-/-}$-mice but not in *Cx43*$^{+/+}$-mice at 4 - 6 mM extracellular Ca^{2+} (Ca_o).
Conclusion: Cx43 deficiency depolarizes $\Delta\Psi_m$ and increases Ca_m at higher Ca_o, ROS production, Ca^{2+} spark frequency, and arrhythmogenesis. All these changes in *Cx43*$^{-/-}$-mice are suppressed by DZX. Thus, with modulation of mK_{ATP}, mCx43 can be involved in the occurrence of arrhythmias.

B-PO02-020

PDE4D MEDIATES DESENSITIZATION OF B-ADRENERGIC RECEPTORS IN THE SINOATRIAL NODE IN HYPERTENSIVE HEART DISEASE

Tristan W. Dorey and Robert A. Rose PhD

Background: Chronotropic incompetence is common in hypertensive heart disease due to impaired β-adrenergic receptor (β-AR) responsiveness of the sinoatrial node (SAN).
Objective: To determine the mechanism for impaired β-AR signaling in the SAN of angiotensin II (AngII) induced hypertensive heart disease.
Methods: C57BL/6 mice were infused with saline or AngII (2.5mg/kg/day) for 21 days to induce hypertensive heart disease. Heart rate (HR) and SAN function in response to the β-AR agonist isoproterenol (ISO) were studied by *in vivo* electrocardiography, in isolated atrial preparations by optical mapping, in isolated SAN myocytes by patch-clamping, and by molecular techniques.
Results: AngII infused mice had impaired HR increases in response to ISO (100mg/kg) *in vivo* (171.1±7.1 vs. 134±9.8 bpm; n=5-6 mice; $P<0.05$) and in isolated atrial preparations (10μM ISO; 160.4±9.7 vs. 96.6±7.8, $n=5$-6 hearts; $P<0.05$). ISO (10μM) induced increases in SAN conduction velocity were also smaller in AngII infused hearts (1.6±0.1 vs. 1.1±0.1 cm/s, $n=5$-6 hearts; $P<0.05$). The effects of ISO (10μM) in isolated SAN myocytes after AngII infusion were impaired as indicated by smaller increases in spontaneous action potential (AP) firing (54.5±4.6 vs. 28.3±2.7 AP/min; $P<0.001$), diastolic depolarization (DD) slope (33.2±3.8 vs. 19.0±3.5 mV/s; $P<0.05$), peak "funny" current (-3.7±0.2 vs. -1.8±0.1 pA/pF; $P<0.05$), and peak L-type Ca^{2+} current (-6.9±1.3 vs. -3.5±0.7 pA/pF; $P<0.05$; $n=7$-15 cells). SAN myocytes from AngII infused mice had diminished cAMP generation in response to ISO (126.5±4.7 vs. 103.7±5.3 nM/1000 cells; $P<0.05$). No differences were seen in the protein expression of β1- or β2-ARs (both $n=6$; $P>0.05$); however, AngII infused mice had increased SAN PDE4 activity (1.4±0.3 vs. 3.9±0.9 pmol/mg/min, $n=5$; $P<0.05$). Total PDE4 expression was unaltered in the SAN of AngII infused mice but localization of PDE4D surrounding both β1- and β2-ARs was increased ($n=6$; $P<0.05$). Acute application of the PDE4 inhibitor rolipram (10μM) normalized ISO (10nM) induced increases in AP firing and DD slope in SAN myocytes (n=8-10) from AngII infused mice.
Conclusion: AngII infusion results in blunted HR responses to β-AR stimulation due to upregulation of PDE4D specifically around β-ARs in the SAN.

B-PO02-021

INCREASED MICROTUBULE DETYROSINATION ENHANCES MECHANO-ARRHYTHMOGENICITY THROUGH TRPA1 IN VENTRICULAR MYOCYTES

Breanne Ashleigh Cameron BS, Jessi J. Bak MSc, Matthew R. Stoyek PhD and T. Alexander Quinn PhD

Background: In hypertension, there is an increased risk of sudden cardiac death, which is associated with acute hemodynamic fluctuations in the presence of ventricular structural remodelling. Increased microtubule network (MTN) density (*via* polymerisation) or stability (*via* post-translational modifications, such as detyrosination or acetylation) may enhance mechano-transduction in this setting and increase the incidence of mechanically-triggered arrhythmias ('mechano-arrhythmogenicity') mediated by TRPA1.
Objective: Determine the impact of alterations in the MTN on mechano-arrhythmogenicity.

Methods: Rabbit LV myocytes paced at 1Hz were rapidly stretched at increasing magnitudes (8-19% increase in sarcomere length over ~112ms) during diastole with carbon fibres. Cells were exposed to paclitaxel to hyperpolymerise and stabilise (*via* increased detyrosination and acetylation) the MTN. Drugs were used in paclitaxel-treated cells to reduce microtubule density (colchicine) or detyrosination (parthenolide), or to block mechano-sensitive TRPA1 channels (HC-030031), and in control cells to increase acetylation (tubacin). Diastolic cell stiffness was measured from stepwise generated force-length curves. MTN density was assessed by immunofluorescence.
Results: In paclitaxel-treated cells, there was a stretch magnitude-dependent threshold (≥13±1% increase in sarcomere length) over which mechano-arrhythmogenicity was greater than in control (13 *vs* 4% of stretches resulted in an arrhythmia; $n=41$ cells, $N=5$ rabbits; $p<0.005$). Arrhythmia incidence in paclitaxel-treated cells was reduced by colchicine (4%; $p<0.005$), parthenolide (6%; $p<0.05$), and HC-030031 (2%; $p<0.0005$), while tubacin applied to control cells did not increase arrhythmia incidence ($n=41$, $N=5$). Paclitaxel increased cell stiffness (45±6 *vs* 30±3nN/μm, $n=25$, $N=5$; $p<0.05$) and MTN density (64±2 *vs* 74±3%, $n=7$, $N=2$; $p<0.05$) compared to control, which was not prevented by colchicine or parthenolide. In control cells, tubacin also increased stiffness (43±5nN/μm, $N=5$, $n=25$; $p<0.05$).
Conclusion: An increase in MTN detyrosination, rather than cell stiffness, MTN density, or MTN acetylation, results in increased mechano-arrhythmogenicity mediated by TRPA1.

B-PO02-022

COMBINING SIMULATION AND MACHINE LEARNING TO ACCURATELY PREDICT ARRHYTHMIC RISK IN POST-INFARCTION PATIENTS

Mary M. Maleckar PhD, Per Magne Florvaag, Vilde Nyrønning Strøm, Charlotte Glinge, Reza Jabbari, Niels Vejlstrup, Thomas Engstrom, Kiril Ahtarovski, Thomas Jespersen, Jacob Tfelt-Hansen DSC, MD, Valeriya Naumova and Hermenegild J. Arevalo PhD

Background: Remodeling post-myocardial infarction (MI) increases arrhythmic risk. Simulations using patient-specific models show promise for prediction of personalized risk but simulations can be computationally- and time-intensive, hindering translation to the clinic.
Objective: We aim to demonstrate that machine learning (ML) algorithms based solely on MI patient geometries can be used to accurately predict arrhythmia occurrence as determined by simulation.
Methods: Computational heart models were constructed from 38 patients 5 days post-MI (Fig A). Arrhythmia induction was attempted via programmed stimulation at 17 sites corresponding to AHA left ventricular segments. We used global myocardial and scar volumes and segment-specific myocardial volume and scar transmurality (geometric features), as input to ML algorithms. One clustering and three classification ML models were trained, *to predict the occurrence of arrhythmia directly from geometric features*. Training was performed on 70% of randomly selected segments, the remaining 30% used for validation. Each model training used a different train/validation segment split.
Results: Stimulation from 120 sites resulted in reentry in 17 patients (Fig B). The best performing model was a neural network, correctly predicting arrhythmia in 87.6% of the cases, on average (+/- 1.3%, Fig C).
Conclusion: Results reveal that combining even established ML methods with simulation can provide key clinical insights with high accuracy, rapidly and efficiently. This work paves the way for our further ML model development to improve accuracy and ultimate use of data-driven simulation for prediction of arrhythmia risk in MI patients.

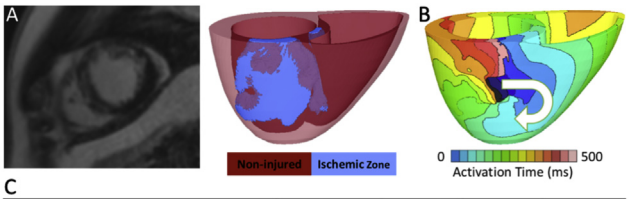

C

Machine Learning Model	Average	Std	Max	Min
K-Means	76.8%	3.0%	83.0%	70.6%
Gaussian Support Vector Machine	85.1%	2.1%	88.7%	80.4%
Decision Tree	85.9%	2.0%	89.2%	80.9%
Neural Network	87.6%	1.3%	89.3%	84.5%

B-PO02-023

ARTIFICIAL INTELLIGENCE PLATFORM FOR STRATIFICATION OF ATRIAL FIBRILLATION PRIOR TO ABLATION

Ana María Sanchez de la Nava MSci, Nina Soto, Jairo López, Tomas Datino MD, Pablo Ávila MD, Esteban Gonzalez-Torrecilla, Angel Arenal Maiz MD, Francisco Fernández-Avilés MD, PhD and Felipe Atienza MD, PhD

Background: Artificial Intelligence (AI) has arisen as a powerful tool for prediction.
Objective: We used an AI-driven platform for the stratification of patients prior to ablation based on Body Surface Potential Mapping (BSPM) recordings and non-invasive electrocardiographic imaging (ECGi).
Methods: Two different coupled algorithms were trained in 2 steps: a) 2-second signals from the BSPM and its corresponding ECGi metrics (N=892) from 150 patients were used to train and validate an 8-layer convolutional network, evaluated using the Mean Absolute Error (MAE), for 5 parameter estimation: highest DF, minimum DF, differential HDF median, mean simultaneous rotors and mean rotor time in percentage; b) the network output was later used to calculate the AF/AF freedom probability at 1-year after ablation using a regression algorithm.
Results: Network performance was evaluated for the prediction of the highest DF (MAE: 0.12), minimum DF (MAE: 0.08), differential HDF median (MAE: 0.11), mean simultaneous rotors (MAE: 0.01) and mean rotor time in percentage (MAE: 1.04) showing good performance for all the parameters. Once the biomarkers were calculated, the regression algorithm resulted in 86.15% specificity and 82.14% sensitivity for predicting ablation outcome. This AI platform can be run and tested in less than 1 minute.
Conclusion: This workflow could be used as a platform to rapidly calculate parameters from the ECGi and, from those, predict the long-term efficacy of the ablation. This algorithm allows patients stratification and clinical interpretation of biomarkers.